Stronger carbon uptake by the ocean in eddy-resolving simulations of global warming

Damien Couespel[a,], Marina Lévy[b], Laurent Bopp [c]*

[a]*NORCE Norwegian Research Centre, Bjerknes Centre for Climate Research, Bergen, Norway*

[b]*Sorbonne Université, LOCEAN-IPSL, CNRS/IRD/MNHN, Paris, France*

[c]*LMD-IPSL, École Normale Supérieure/PSL University, CNRS, École Polytechnique, Sorbonne Université, Paris, France*

[*]*Corresponding author: daco@norceresearch.no*

Keypoints

1. We conduct idealized simulations of global warming using increasingly finer horizontal resolutions, with an ocean-biogeochemical model.
2. Oceanic carbon-concentration and carbon-climate feedbacks are highly influenced by resolution.
3. It primarily stems from how the overturning circulation's mean state depends on resolution, as well as how it responds to global warming.

Abstract

Today, the ocean absorbs ~25 % of the human-induced carbon emissions. Earth System Models (ESMs) indicate that the absorption increases by 0.79 ± 0.07 PgC per ppm of atmospheric CO2 increase (carbon-concentration feedback), but diminishes by -17.3 ± 5.5 PgC per degree of warming (carbon-climate feedback). Due to limited computational capacity, ESMs parameterize flows at scales smaller than their horizontal grid resolution, typically ~1 °. We conduct simulations of global warming using increasingly finer horizontal resolutions (from 1 ° to 1/27 °), with an ocean-biogeochemical model, in an idealized mid-latitude double-gyre circulation. Our findings demonstrate that these ocean carbon cycle feedbacks are highly influenced by resolution. This sensitivity primarily stems from how the overturning circulation's mean state depends on resolution, as well as how it responds to global warming. Although being a fraction of the intricate response to climate change, it emphasizes the significance of an accurate representation of small-scale ocean processes to better constrain the future ocean carbon uptake.

Plain language summary

Today, the ocean absorbs ~25 % of the carbon emissions caused by human activities. This carbon sink is primarily driven by the increase of CO_2 in the atmosphere, but it is also influenced by physical changes in the ocean's properties. Earth System Models (ESMs) are used to project the future of the ocean carbon sink. Due to limited computational capacity, ESMs need to parameterize flows occurring at scales smaller than their horizontal grid resolution, typically ~1 °. To address these computational limitations, we employ an ocean biogeochemical model in an idealized setup representing a mid-latitude double-gyre circulation. We conduct simulations of global warming using increasingly finer horizontal resolutions (from 1 ° to 1/27 °). Our findings

demonstrate that the ocean carbon uptake is highly influenced by resolution. This sensitivity primarily stems from how the overturning circulation's mean state depends on resolution, as well as how it responds to global warming. Although our results capture only a fraction of the intricate oceanic response to climate change, they emphasize the significance of accurately representing the role of small-scale ocean processes to better constrain the future evolution of ocean carbon uptake.

1 Introduction

By absorbing 25 % of anthropogenic carbon emissions (Friedlingstein et al., 2022), the ocean plays a crucial role in determining the rate at which CO_2 increases in the atmosphere, thus influencing the pace of climate change. This carbon uptake is primarily attributed to the rise in atmospheric CO_2 and its impact on the partial pressure equilibrium of CO_2 at the air-sea interface. However, this absorption is modulated by changes in oceanic physics, particularly the warming of surface waters and increased ocean stratification, both of which tend to decrease this flux (Sarmiento et al., 1998; Sarmiento and Le Quéré, 1996; Maier-Reimer et al., 1996). Through enhancing or reducing the ocean carbon sink, changes in the ocean carbon cycle act as a negative or positive feedback on the Earth's climate, respectively. Understanding the ocean's capacity to mitigate or amplify human-induced climate change is essential for projecting the future climate trajectory.

Two metrics have been established to measure the ocean carbon sink response to increasing atmospheric CO_2 and climate change: the carbon-concentration and carbon-climate feedback parameters (Katavouta and Williams, 2021; Arora et al., 2020; Schwinger et al., 2014; Boer and Arora, 2013; Roy et al., 2011; Friedlingstein et al., 2006). The former quantifies the ocean carbon cycle's response to the rise in atmospheric CO_2 levels, while the latter measures its response to changes in the physical climate. These metrics are typically evaluated using Earth System Models (ESMs) and idealized climate change scenarios in which atmospheric CO_2 increases at 1 % per year (Eyring et al., 2016). Arora et al. (2020) utilized 11 ESMs from the Coupled Model Intercomparison Project Phase 6 (CMIP6) to assess the carbon-concentration feedback at $0.79 \pm 0.07\,\mathrm{Pg\,C\,ppm^{-1}}$ and the carbon-climate feedback at $-17.3 \pm 5.5\,\mathrm{Pg\,C\,°C^{-1}}$.

One significant limitation of ESMs arises from computational constraints and the use of coarse grid resolution, which lead to an inadequate representation of transient eddies and flows of scales below 100 km (Gent and McWilliams, 1990). To overcome these limitations, coarse-resolution ESMs (1 ° or coarser) use sub-grid parameterizations, which enables capturing certain key aspects of the ocean carbon cycle. These models reproduce reasonably well the global net carbon uptake over the historical period (Hauck et al., 2020; Séférian et al., 2020; Bronselaer et al., 2017) and replicate large-scale carbon uptake/outgassing patterns, as well as key carbon cycle drivers like primary production (Séférian et al., 2020), mixed layer depth (Fu et al., 2022; Séférian et al., 2019), and carbon subduction/obduction (Davila et al., 2022; Lévy et al., 2013; Sallée et al., 2012). Nonetheless, these processes and their response to climate change are sensitive to sub-grid process representation (Brett et al., 2023; Couespel et al., 2021; Bahl et al., 2020; Resplandy et al., 2019; Harrison et al., 2018; Balwada et al., 2018; Mahadevan et al., 2011), potentially introducing biases into current estimates of carbon uptake and the carbon-concentration and carbon-climate feedbacks. In this study, we examine how eddy resolution influences the ocean's carbon sink response to future global warming.

Explicitly resolving eddies in ocean models is known to impact the positioning of western boundary currents (Chassignet and Xu, 2017; Lévy et al., 2010; Chassignet and Marshall, 2008), alter the Meridional Overturning Circulation's strength (MOC, Hirschi et al., 2020; Roberts et al., 2020), and increase stratification (du Plessis et al., 2017; Karleskind et al., 2011; Lévy et al., 2010; Chanut et al., 2008). These changes affect the transport of heat and tracers, including carbon (Swierczek et al., 2021; Uchida et al., 2020; Chen et al., 2019; Uchiyama et al., 2017; Lévy et al., 2012). Furthermore, eddy activity may evolve with global warming (Beech et al., 2022; Martínez-Moreno et al., 2021; Oliver et al., 2015), further influencing ocean circulation and carbon transport. Investigating these effects resulting from resolved eddies has recently started within global warming scenarios (Hewitt et al., 2022; Rackow et al., 2022; van Westen and Dijkstra, 2021; Chang et al., 2020), generally using resolutions not finer than 1/10 °, and to the best of our knowledge, not in terms of their implications for ocean carbon cycle feedbacks.

This study assesses the impact of explicitly representing eddies and horizontal flows with scales ranging from 10 km to 100 km on the response of the oceanic carbon uptake to increasing CO_2 and global warming. The subsequent section outlines the idealized setup employed in this study, followed by the presentation of results and concluding with a discussion regarding the implications for climate projections using ESMs.

2 Methods

2.1 Models and configurations

Ocean physics are simulated with the primitive-equation ocean model NEMO (Madec et al., 2017) coupled to the biogeochemical model LOBSTER (Lévy et al., 2012, 2005), in which the carbon cycle as been activated (Sec. S1 and Tab. S2). The domain is a closed square basin on a mid-latitude β-plan. It is 3180 km wide and long and 4 km deep, bounded by vertical walls and by a flat bottom with free slip boundary conditions. A double-gyre circulation is set up by analytical zonal forcings (wind stress, net heat flux and freshwater flux) which vary seasonally between winter and summer extrema. The net heat flux comprises a restoration toward a zonal atmospheric temperature profile and a solar radiation allowed to penetrate within the water column. CO_2 is exchanged with the atmosphere following Wanninkhof (1992, Eq. 8) and forced with a prescribed atmospheric partial pressure of CO_2 (pCO_2).

We use three horizontal resolutions: 106 km (1 °), 12 km (1/9 °) and 4 km (1/27 °). For each resolution, time steps, numerical schemes and isopycnal/horizontal diffusion are adapted (Tab. S1). For the 1 ° resolution configurations, we used the Gent and McWilliams (1990, GM hereafter) eddy parameterization. This parameterization relies on two coefficients, an isopycnal diffusion coefficient (k_{iso}) and a GM coefficient (k_{gm}). For testing the sensitivity to the GM parameterization, we used five combinations of the isopycnal diffusion and GM coefficients: (1) 500 m^2s-1, (2) 1000 m^2s-1 and (3) 2000 m^2s-1 for both parameters and (4) 500 m^2s-1 and (5) 2000 m^2s-1 for the isopycnal diffusion parameter but keeping the GM coefficient at 1000 m^2s-1. We thus end up with seven different configurations: five eddy-parameterized at a coarse resolution (1 °) and two eddy-resolving at fine resolutions (1/9 ° and 1/27 °). In the following, results from the eddy-parameterized coarse resolution configurations are synthesized by showing the average ±1 standard deviation across the five different configurations. For the higher resolution configurations, there is no momentum nor tracer diffusion but a minimal bi-Laplacian tracer diffusion at 1/27 °. Contrary to the 1/27 ° configuration, the qualifier "eddy-permitting" is probably more appropriate for the 1/9 ° configuration. Nevertheless, to simplify and as the emphasis is put on the differences between the 1 ° resolution and the finer ones, we use the term eddy-resolving for both.

The model and configurations are similar to the one described in Couespel et al. (2021) and were derived from prior studies (Resplandy et al., 2019; Lévy et al., 2012; Krémeur et al., 2009). The key elements have been outlined above. For further details, we refer to the aforementioned papers.

2.2 The different simulations and experimental design

After a 100 years spin up at each resolution initialized with the same physical and biogeochemical state (from a 2000 year spin-up at coarse resolution), 4 different experiments are conducted. They are forced by different combinations of atmospheric temperature and atmospheric pCO_2 (see Fig. 1a,b). (1) The control simulation (CTL) is the continuation of the spin-up, with temperature keeping a seasonal cycle and atmospheric pCO_2 staying constant. (2) In the biogeochemical simulation (BGC), atmospheric pCO_2 increases by 1% every year, but atmospheric temperature stays constant (with a seasonal cycle). (3) In the radiative simulation (RAD), atmospheric temperature increases by 0.04 °C every year (with a seasonal cycle), while atmospheric pCO_2 is kept constant. (4) In the coupled simulation (COU), both atmospheric pCO_2 and atmospheric temperature increase by 1 % and 0.04 °C every year, respectively. The term coupled (COU) is to be coherent with the naming used with ESMs. However, here, atmospheric temperature and atmospheric pCO_2 are not radiatively coupled. Besides, despite the use of the term "atmospheric", there is no atmospheric model.

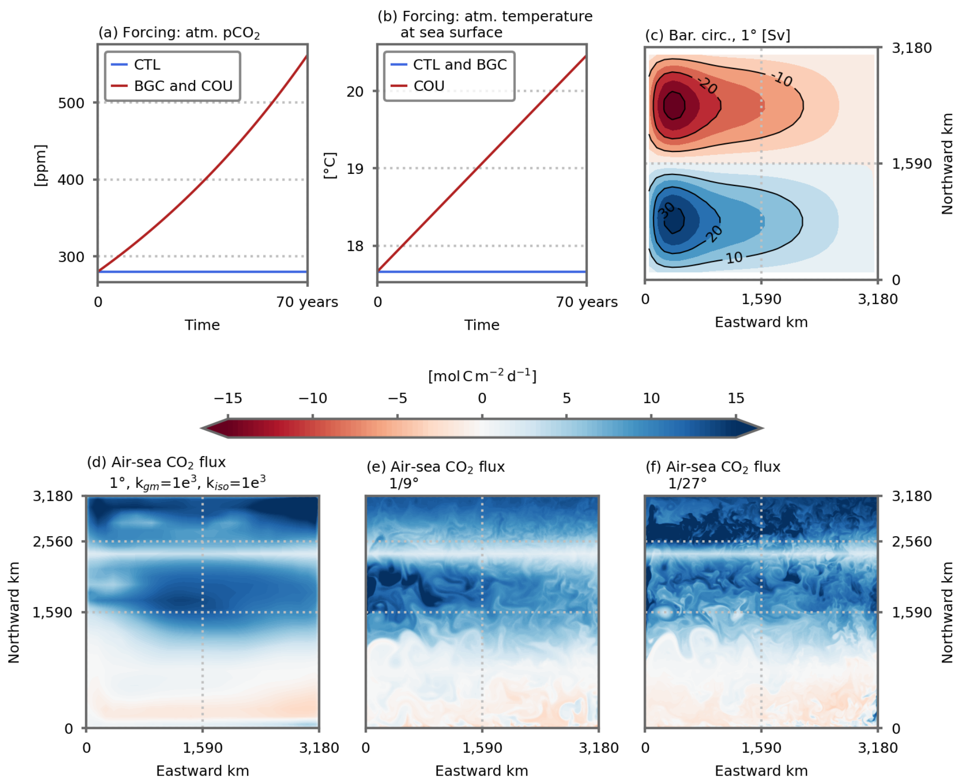

Figure 1. Overview of the configurations and simulations. **(a)** Time series of the analytical atmospheric pCO_2 [ppm] forcing for the CTL simulation (blue line) and for the BGC and COU simulations (red line). **(b)** Time series of the mean analytical atmospheric temperature [°C] forcing for the CTL and BGC simulations (blue line) and for the COU simulation (red line). Shown is the atmospheric temperature average yearly and on the domain. **(c)** Barotropic circulation [Sv] over the model domain (average of the five 1 ° resolution CTL simulations). Air-sea carbon flux [$\mathrm{mol\,C\,m^2\,d^{-1}}$] on March, 3^{nr} in **(d)** the 1 ° (k_{gm}=1e^3 and k_{iso}=1e^3), **(e)** the 1/9 ° and **(f)** the 1/27 ° CTL simulations.

The main features of the model's solution comprise a western boundary current separating a subtropical gyre outgassing carbon in the south of the domain from a subpolar gyre uptaking carbon in the north (Fig. 1). A rather classic MOC is simulated with northward transport in the upper ocean (above $\simeq$ 250 meters), downwelling in the north and then southward transport at depth. In the northernmost part of the domain (2,560-3,180 northward km), deep convection occurs in winter with mixed layer depth reaching 1,000 meters and more. As resolution increases, mesoscale eddies and filamentary structures emerge in the air-sea carbon flux (Fig. 1d-f). Dissolved Inorganic Carbon (DIC) concentration increases with depth (Fig. 2a). With increasing resolution, vertical profiles are more homogeneous. The vertical gradients are weaker and DIC concentration are lower at

250-1,250 metres. The equilibrium states have been further described in Couespel et al. (2021).

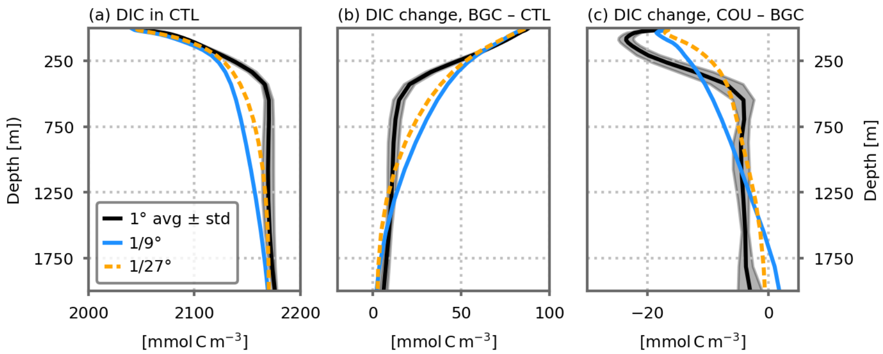

Figure 2. Dissolved inorganic carbon concentration (DIC, [mmol C m^{-3}]) vertical profiles spatially averaged for the three resolutions. **(a)** DIC profiles in the CTL simulation. Change in DIC between **(b)** the BGC and CTL simulations and **(c)** the COU and BGC simulations. All profiles are averaged on the 10 last years of the simulations. The 1 ° resolution profiles shows the average of the five 1 ° configurations. Shading indicates ± 1 inter-model standard deviation.

2.3 Feedback metrics and carbon budget

The responses of the ocean carbon cycle to 1) the increase in atmospheric pCO_2 and 2) the change in ocean physical properties are respectively quantified by the carbon-concentration and carbon-climate feedbacks. Following the traditional BGC-COU approach (Arora et al., 2020), they are defined as:

$$\text{carbon-concentration feedback:} \quad \beta = \frac{\Delta C_{BGC}}{\Delta C_{atm}} \qquad \textbf{Equation } 1.$$

$$\text{carbon-climate feedback:} \quad \gamma = \frac{\Delta C_{COU} - \Delta C_{BGC}}{\Delta T_{atm}} \qquad \textbf{Equation } 2.$$

ΔC_{COU} and ΔC_{BGC} are the cumulative changes in carbon uptake in the COU and BGC simulations relative to the CTL simulation, ΔC_{atm} is the accumulation of CO_2 in the atmosphere and ΔT_{atm} is the change in atmospheric temperature.

The feedback metrics are related to CO_2 uptake, its response to warming and the distribution of DIC in the ocean interior. Locally, the DIC budget is : $-\vec{\nabla}\cdot(\vec{u}\cdot DIC) + L(DIC) + \partial_z(k\cdot\partial_z DIC) + B(DIC) + fCO_2 = \partial_t DIC$. $\vec{\nabla}\cdot(\vec{u}\cdot DIC)$ is the divergence of the advective fluxes, $\partial_z(k\cdot\partial_z DIC)$ is the vertical diffusion term, $L(DIC)$ is the isopycnal diffusion, $B(DIC)$ represents the biological sources and sinks of DIC and $fCO2$ the air-sea CO_2 flux when at the surface. u is the total velocity and includes the bolus velocity of the GM parametrization at coarse resolution. Integrated on the upper ocean (surface to 250 metres depth) and along the 70 years of the simulations, the local DIC budget becomes:

$$\begin{aligned}
\textbf{CO}_\textbf{2}\textbf{ uptake}: \int_0^{70} \langle fCO_2 \rangle \,\mathrm{dt} = & \int_0^{70} \oint \vec{u}\cdot DIC \,\mathrm{ds}\,\mathrm{dt} && \textbf{Advection} \\
- & \int_0^{70} \langle k\cdot\partial_z DIC_{|250m} \rangle \,\mathrm{dt} - \int_0^{70years} \langle L(DIC) \rangle \,\mathrm{dt} && \textbf{Diffusion} \\
+ & \int_0^{70} \langle B(DIC) \rangle \,\mathrm{dt} && \textbf{Biological sources and sinks} \\
+ & \Delta \langle DIC \rangle && \textbf{Change in DIC stock}
\end{aligned}$$

Equation 3.

The bracket stands for the volume integral on the upper ocean or the horizontal integral at the surface for the CO_2 uptake and at 250 metres depth for the vertical diffusion term. The first term on the right side is the integral of the advective fluxes entering/exiting the upper ocean, i.e. the vertical DIC advective flux at 250 metres depth, here. A similar budget is computed for the lower ocean (250 metres depth to bottom). In that case, the CO_2 uptake by the ocean term is null. These budgets have been computed at each time step of all the simulations. Furthermore, particularly for relating the advective transport with the MOC, the budget is also computed with the upper and lower ocean being divided latitudinally in 3 regions representing the subtropical gyre, the subpolar gyre and the convection zone (respectively 0-1,590, 1,590-2,560 and 2,560-3,180 northward km, see Sec. S2)

The differences in the DIC distribution and budget between the BGC and CTL simulations give some insights about the drivers of the carbon-concentration feedback, while the differences between the COU and BGC simulations tell us about the carbon-climate feedback. The extra carbon added to the system in response to the increasing atmospheric pCO_2 is the anthropogenic carbon. The change between the BGC and CTL simulation thus show the anthropogenic DIC distribution and budget. The difference between the COU and BGC simulation include the response of the anthropogenic DIC to warming as well as the response of the natural DIC. To disentangle one from another, we use the RAD simulation. The differences between the RAD and CTL simulations reveal the response of natural DIC to warming (Fig. S2a), while the remainder reveal the response of anthropogenic DIC to warming (Fig. S2b).

3 Results

3.1 Sensitivity of ocean carbon uptake to resolution

All along the 70 years of the COU simulation, carbon accumulates in the ocean (Fig. 3a). This accumulation is driven by the rise in atmospheric pCO_2, slightly offset by the response to warming-induced changes in ocean circulation and biogeochemistry (Fig. 3b, c). At coarse resolution, the carbon-concentration feedback is $0.18 \pm 0.01\,\mathrm{mol\,C\,m^{-2}\,ppm^{-1}}$ while the carbon-climate feedback is $-5.42 \pm 0.28\,\mathrm{mol\,C\,m^{-2}\,°C^{-1}}$. As a consequence, DIC concentration increases in the BGC simulation as compared with the CTL simulation (Fig. 2b), and decreases in the COU simulation as compared with the BGC simulation (Fig. 2c). The strongest changes take place in the first 500 meters.

With finer resolution, the ocean uptakes about 30 % more carbon (Fig. 3a). 87 % (1/9 °) and 78 % (1/27 °) of this extra uptake is caused by a stronger response to atmospheric pCO_2 increase (Fig. 3b). The remainder is explained by a weaker decline in uptake because of warming (Fig. 3c). The carbon-concentration feedback is stronger (0.22 and 0.21 $\mathrm{mol\,C\,m^{-2}\,ppm^{-1}}$ for the 1/9 ° and 1/27 ° resolution, respectively) while the carbon-climate feedback is weaker (-4.93 and -4.23 $\mathrm{mol\,C\,m^{-2}\,°C^{-1}}$ for the 1/9 ° and 1/27 ° resolution, respectively). As a consequence, there is a stronger DIC concentration increase in the BGC simulation (as compared with the CTL simulation, Fig. 2b), notably between at the subsurface (250-1250 meters).

3.2 Resolution-induced changes in the carbon-concentration feedback

The carbon-concentration feedback depends on the ability of the ocean to transport anthropogenic carbon to the deep ocean, so that the uptake at the surface is maintained (Figs. 2b and 4a). Once in the ocean, anthropogenic carbon is advected northward by the upper limb of the MOC. It is then transfered downwards (through mixing and advection) in the high latitude part of the domain (mainly the convection zone) before being advected back southward. A small fraction is then advected upward back to the surface (Fig. S1). Diffusive flux participate in this downward flux of carbon by counteracting against the gradients (Fig. 2b). About 90 % of the diffusion occurs in the convection zone.

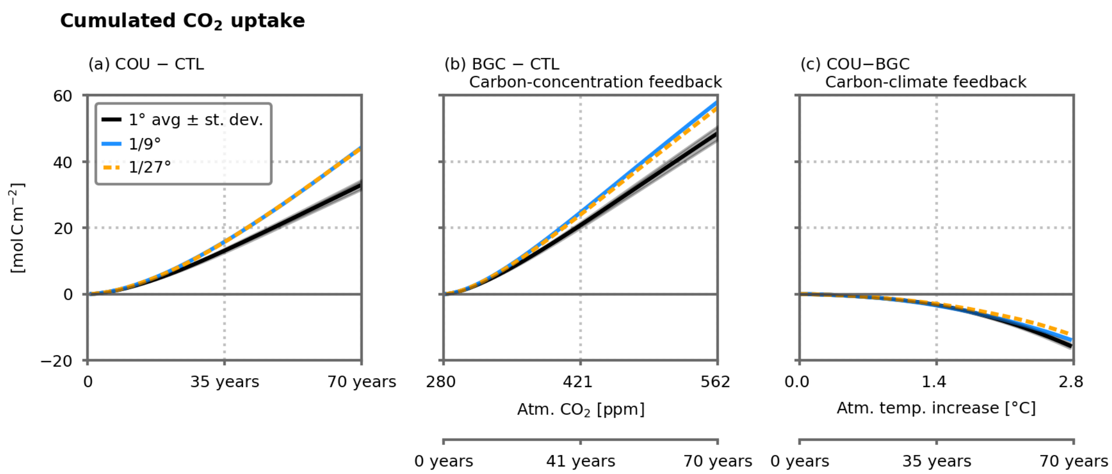

Figure 3. (a) Time series of the change in cumulated carbon uptake [mol C m^{-2}] COU simulations for the three resolutions. **(b)** Change in cumulated carbon uptake [mol C m^{-2}] in the BGC simulations vs. atmospheric pCO_2 [ppm] for the three resolution. **(c)** Change in cumulated carbon uptake [mol C m^{-2}] in the COU simulations relative to the BGC simulations vs. change in atmospheric temperature [°C] in the COU simulation. The 1 ° resolution lines shows the average of the five 1 ° configurations. Shading indicates ±1 inter-model standard deviation.

With finer resolution, more anthropogenic carbon is transported and stored at depth (Figs. 2b and 4a)). Below 250 metres, there is about 90 extra Tmol C stored in the finer resolution (Fig. 4a), mostly in the subtropical gyre (Fig. S1). 97-79 extra Tmol C are absorbed at the air-sea interface. This extra carbon is advected northward at the surface, downward in the convection zone and then southward to ultimately being accumulated in the sub-surface of the subtropical gyre. Advection transports more anthropogenic carbon to the sub-surface at finer resolution. This more vigorous advection is related to the stronger MOC (Couespel et al. (2021, Fig. A8), MOC increasing from 1.75 Sv at 1 ° to 3.14 Sv at 1/9 ° and 2.94 Sv at 1/27 °). The stronger advection is partially balanced by a weaker mixing at finer resolution, resulting in less anthropogenic carbon transported to the sub-surface at finer resolution. This is likely related to the weaker gradient at finer resolution (Fig. 2b).

3.3 Resolution-induced changes in the climate-carbon feedback

The climate change induced decrease in carbon uptake is a consequence of decreasing CO_2 solubility (induced by warming) and of the balance between changes in DIC transport, leaving more DIC at depth, and the decline in DIC consumption by primary production at the surface (Fig. 4b). The major change is the decline in biological consumption of DIC at the surface, mirrored by a decline in organic matter remineralization at depth, resulting in less carbon exported to the deep ocean. It mostly happens in the subpolar gyre and the convection zone, which are also the areas with the stronger decline in primary production (Fig. S1 and Couespel et al., 2021) The second largest change is the increase in downward diffusive fluxes transporting more carbon from the surface to the deep ocean, mostly in the convection zone (Fig. S1). It is likely related to the shallowing of the mixed layer depth (Couespel et al., 2021, Fig. A9). Changes in advection have minor impact in terms of transport between the surface and deep oceans. However, this comes from a compensation between a strong decrease in upward and downward advective fluxes (Fig. S1) driven by the MOC decline (Couespel et al., 2021, Fig. A8). Changes in the DIC transport results from a compensation between a decline in the upward transport of natural DIC and the downward transport of anthropogenic DIC (Fig. S2). The decrease in upward transport of natural DIC, paired with the decrease in upward transport of nutrients, is the counterpart to the decrease in biological consumption. The two almost offset each other, although more carbon is left in the deep ocean.

The climate change induced responses of DIC transport and biological source and sink of DIC are weaker at finer resolution (Fig. 4b). A weaker decrease in primary production leads to a weaker decline in DIC consumption

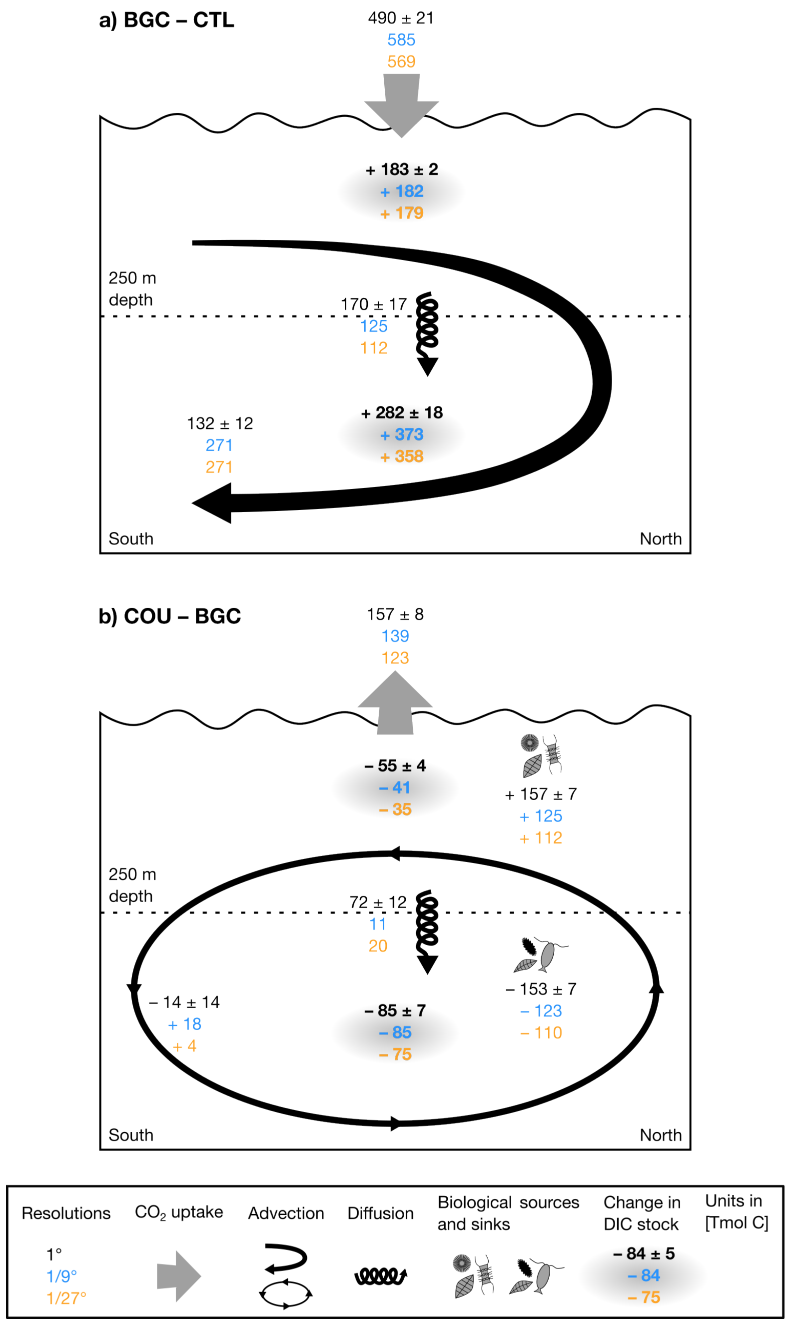

Figure 4. Differences in dissolved inorganic carbon (DIC) budgets (integrated over space and time) in the upper and lower ocean (resp. above and below 250 meters depth) for the three resolutions (see Eq. 3). a) Differences between the BGC and CTL simulations. b) Differences between the COU and BGC simulations. Bold numbers stand for changes in DIC stocks. Thin number for differences in CO_2 uptake, physical transport (advection, diffusion) and the biological sources and sinks. The CO2 uptake arrow indicate the direction of the flux (uptake or outgas). For advection and diffusion terms, positive values stand for a DIC transport from upper to lower ocean. The arrow indicate the direction of the difference of the fluxes. For advection, it is a synthetic view of figure S1. The 1 ° resolution numbers are the average of the five 1 ° configurations ±1 inter-model standard deviation.

at the surface, as well as a weaker decline in remineralization at depth. The weaker increase in the downward diffusive flux may be related to a weaker shallowing of the mixed layer depth (Couespel et al., 2021, Fig. A9). However, it should be noted that the finer resolution simulations do not include isopycnal mixing that is present in the coarse resolution simulations and added to the diffusive flux. Finally, advection changes result in more (and not less) carbon left in the deep ocean in the 1/9 ° and 1/27 ° resolution simulations. This also stems from a compensation between decreases in the upward and downward advective fluxes, although the decrease is weaker at finer resolution (Fig. S1). This is likely related to the weaker decline in the MOC at finer resolution (Couespel et al., 2021, Fig. A8). As for the coarse resolution, changes in DIC transport arise from the decline in the upward transport of natural DIC (compensating the decline in DIC consumption) and the decline in the downward transport of anthropogenic DIC (Fig. S2).

4 Discussion and conclusions

Using a wind and buoyancy driven double-gyre model to run idealized biogeochemically coupled simulations of global warming, we show that ocean carbon uptake is sensitive to horizontal grid resolution. It is about 35 % larger at eddy resolution. Ocean carbon uptake results from the combination of direct uptake of human emitted CO_2 (carbon-concentration feedback) as well the negative feedback induced by the carbon-cycle response to global warming (carbon-climate feedback). About 78–87 % of the larger carbon uptake at high resolution results from a stronger direct uptake of anthropogenic carbon induced by a stronger transport at depth through the MOC. The remainder comes from a weaker negative carbon-climate feedback, likely related to a weaker decline in the MOC and primary production in response to warming (Fig. 4 and Couespel et al., 2021).

The carbon-concentration and carbon-climate feedbacks evaluated at coarse resolution in this study are in the range of previous estimates from ESMs. In the North Atlantic, the region most similar to our idealized setting, they are respectively estimated to be about 1 to 10 $\mathrm{g\,C\,m^{-2}\,ppm^{-1}}$ and -50 to -300 $\mathrm{g\,C\,m^{-2}\,°C^{-1}}$ in simulations run with ESMs (Katavouta and Williams, 2021, Fig. 2 and Roy et al., 2011, Fig. 10a and Fig. 11a). In this study, at coarse resolution, the feedbacks are respectively 2.16 ± 0.12 $\mathrm{g\,C\,m^{-2}\,ppm^{-1}}$ and 65.04 ± 3.36 $\mathrm{g\,C\,m^{-2}\,°C^{-1}}$. In ESMs, the global ocean carbon-concentration and carbon-climate feedbacks vary respectively from 0.8 to 1.1 $\mathrm{Pg\,C\,ppm^{-1}}$ and from -4.4 to -12.4 $\mathrm{Pg\,C\,°C^{-1}}$ (Arora et al., 2020). In this study, the coarse resolution feedbacks, are respectively 0.78 ± 0.04 $\mathrm{Pg\,C\,ppm^{-1}}$ and -23.48 ± 1.21 $\mathrm{Pg\,C\,°C^{-1}}$, when multiplied by the global ocean area.

In line with prior studies (Brown et al., 2021; Katavouta and Williams, 2021; Ridge and McKinley, 2020; Iudicone et al., 2016; Nakano et al., 2015), our results highlight the importance of having a reliable MOC for projecting future anthropogenic carbon uptake by the ocean. Indeed, we found that in the fine resolution simulation, the stronger MOC implies a stronger transport of anthropogenic carbon at depth and thus a stronger carbon-concentration climate feedback while a weaker MOC decline was associated with a weaker carbon-climate feedback. Such positive correlations between the pre-industrial MOC and the carbon-concentration feedback as well as between the MOC decline and the carbon-climate feedback have been identified in the latest ESMs (Katavouta and Williams, 2021), although not in previous generations (Roy et al., 2011). Our model behaviour is unusual: the finer resolution simulations have a stronger carbon-concentration feedback and a weaker carbon-climate feedback, while the opposite is found in ESMs projections (Arora et al., 2020). This is likely related to the unusual behaviour of the MOC in our simulations: the stronger MOC at finer resolution experiences a weaker decline, while ESMs with a stronger MOC usually project a stronger decline (Roberts et al., 2020; Jackson et al., 2020; Chang et al., 2020; Winton et al., 2014; Gregory et al., 2005).

There are two areas for improvement in the MOC: its mean state and its response to global warming. Our results suggest that addressing the effect of sub-grid processes on the mean state only could largely correct for the resolution-related uncertainty in carbon uptake and induced climate feedbacks. The improved representation of the MOC can be achieved by several solutions that are currently being explored: finer resolution simulations (Yeager et al., 2021; van Westen and Dijkstra, 2021; Chang et al., 2020; Gutjahr et al., 2019; Haarsma et al., 2016), the implementation of improved parametrization schemes Bachman (2019); Jansen et al. (2019); Mak et al. (2018), or the use of statistical approaches (Barthélémy et al., 2022; Sonnewald et al., 2021; Zanna and

Bolton, 2020; Bolton and Zanna, 2019).

In this work, we identified resolution related uncertainties in the projection of future ocean carbon uptake in an idealized regional setting. Many other features may contribute to the sensitivity of ocean carbon uptake to resolution. Changes in the MOC may also be driven by freshwater input (Bras et al., 2021; Jackson et al., 2020), driven by changes in wind stress pattern (Yang et al., 2020), or related to changes in adjacent regions and involving the formation of different water masses (Lique and Thomas, 2018; Bronselaer et al., 2016; Delworth and Zeng, 2008). Carbon uptake is also dependent on the biological carbon pump and the vast number of interconnected processes involved (Henson et al., 2022), whose representation varies among the models (Séférian et al., 2020; Laufkötter et al., 2015). The North Atlantic is the oceanic regime closest to our configurations, but other regions have significant contributions to the global ocean carbon cycle feedbacks (Katavouta and Williams, 2021). For example, the Southern Ocean alone accounts for 40% of the total anthropogenic carbon uptake (DeVries, 2014). The more realistic configurations and the more complex global warming scenario developed in the CMIP6 (and subsequent MIPs) framework would enable these different elements to be explored. The uncertainties linked to the resolution in climate models just start to be explored. The sensitivity of ocean carbon uptake projections to resolution raises concerns about the sensitivity of related climate change issues such as heat uptake and transport (Bronselaer and Zanna, 2020; Chen et al., 2019) or ocean acidification (Kwiatkowski et al., 2020).

Acknowledgements

This research was supported by Chaire Channel ENS. DC acknowledges the EU-funded project OceanICU (101083922). This work used HPC resources from GENCI–IDRIS (Grants 2016-i2016017608, 2016-A0010107608, 2018-A0040107608 and 2019-A0070107608). The authors thank Christian Ethé and Claude Talandier for helping to adapt model configuration.

Code availability

Python scripts used for analysing the model's outputs and for producing the figures are available online at https://github.com/damiencouespel/article-gyre-carbon-diagnostics

References

Pierre Friedlingstein, Matthew W. Jones, Michael O'Sullivan, Robbie M. Andrew, Dorothee C. E. Bakker, Judith Hauck, Corinne Le Quéré, Glen P. Peters, Wouter Peters, Julia Pongratz, Stephen Sitch, Josep G. Canadell, Philippe Ciais, Rob B. Jackson, Simone R. Alin, Peter Anthoni, Nicholas R. Bates, Meike Becker, Nicolas Bellouin, Laurent Bopp, Thi Tuyet Trang Chau, Frédéric Chevallier, Louise P. Chini, Margot Cronin, Kim I. Currie, Bertrand Decharme, Laique M. Djeutchouang, Xinyu Dou, Wiley Evans, Richard A. Feely, Liang Feng, Thomas Gasser, Dennis Gilfillan, Thanos Gkritzalis, Giacomo Grassi, Luke Gregor, Nicolas Gruber, Özgür Gürses, Ian Harris, Richard A. Houghton, George C. Hurtt, Yosuke Iida, Tatiana Ilyina, Ingrid T. Luijkx, Atul Jain, Steve D. Jones, Etsushi Kato, Daniel Kennedy, Kees Klein Goldewijk, Jürgen Knauer, Jan Ivar Korsbakken, Arne Körtzinger, Peter Landschützer, Siv K. Lauvset, Nathalie Lefèvre, Sebastian Lienert, Junjie Liu, Gregg Marland, Patrick C. McGuire, Joe R. Melton, David R. Munro, Julia E. M. S. Nabel, Shin-Ichiro Nakaoka, Yosuke Niwa, Tsuneo Ono, Denis Pierrot, Benjamin Poulter, Gregor Rehder, Laure Resplandy, Eddy Robertson, Christian Rödenbeck, Thais M. Rosan, Jörg Schwinger, Clemens Schwingshackl, Roland Séférian, Adrienne J. Sutton, Colm Sweeney, Toste Tanhua, Pieter P. Tans, Hanqin Tian, Bronte Tilbrook, Francesco Tubiello, Guido R. van der Werf, Nicolas Vuichard, Chisato Wada, Rik

Wanninkhof, Andrew J. Watson, David Willis, Andrew J. Wiltshire, Wenping Yuan, Chao Yue, Xu Yue, Sönke Zaehle, and Jiye Zeng. Global Carbon Budget 2021. *Earth System Science Data*, 14(4):1917–2005, April 2022. ISSN 1866-3508. doi: 10.5194/essd-14-1917-2022.

Jorge L Sarmiento, Tertia M C Hughes, Ronald J Stouffer, and Syukuro Manabe. Simulated response of the ocean carbon cycle to anthropogenic climate warming. *Nature*, 393(6):245–249, 1998. doi: 10.1038/30455.

Jorge L. Sarmiento and Corinne Le Quéré. Oceanic Carbon Dioxide Uptake in a Model of Century-Scale Global Warming. *Science*, 274(5291):1346–1350, November 1996. doi: 10.1126/science.274.5291.1346.

Ernst Maier-Reimer, Uwe Mikolajewicz, and Arne Winguth. Future ocean uptake of CO2: Interaction between ocean circulation and biology. *Climate Dynamics*, 12(10):711–721, 1996. ISSN 09307575. doi: 10.1007/s003820050138.

Anna Katavouta and Richard G. Williams. Ocean carbon cycle feedbacks in CMIP6 models: Contributions from different basins. *Biogeosciences*, 18(10):3189–3218, May 2021. ISSN 1726-4189. doi: 10.5194/bg-18-3189-2021.

Vivek K. Arora, Anna Katavouta, Richard G. Williams, Chris D. Jones, Victor Brovkin, Pierre Friedlingstein, Jörg Schwinger, Laurent Bopp, Olivier Boucher, Patricia Cadule, Matthew A. Chamberlain, James R. Christian, Christine Delire, Rosie A. Fisher, Tomohiro Hajima, Tatiana Ilyina, Emilie Joetzjer, Michio Kawamiya, Charles D. Koven, John P. Krasting, Rachel M. Law, David M. Lawrence, Andrew Lenton, Keith Lindsay, Julia Pongratz, Thomas Raddatz, Roland Séférian, Kaoru Tachiiri, Jerry F. Tjiputra, Andy Wiltshire, Tongwen Wu, and Tilo Ziehn. Carbon–concentration and carbon–climate feedbacks in CMIP6 models and their comparison to CMIP5 models. *Biogeosciences*, 17(16):4173–4222, August 2020. ISSN 1726-4170. doi: 10.5194/bg-17-4173-2020.

Jörg Schwinger, Jerry F. Tjiputra, Christoph Heinze, Laurent Bopp, James R. Christian, Marion Gehlen, Tatiana Ilyina, Chris D. Jones, David Salas-Mélia, Joachim Segschneider, Roland Séférian, and Ian Totterdell. Nonlinearity of ocean carbon cycle feedbacks in CMIP5 earth system models. *Journal of Climate*, 27(11): 3869–3888, 2014. ISSN 08948755. doi: 10.1175/JCLI-D-13-00452.1.

G. J. Boer and V. K. Arora. Feedbacks in emission-driven and concentration-driven global carbon budgets. *Journal of Climate*, 26(10):3326–3341, May 2013. ISSN 08948755. doi: 10.1175/JCLI-D-12-00365.1.

Tilla Roy, Laurent Bopp, Marion Gehlen, Birgit Schneider, P Cadule, Thomas L Frölicher, Joachim Segschneider, Jerry Tjiputra, C Heinze, and Fortunat Joos. Regional impacts of climate change and atmospheric CO2 on future ocean carbon uptake: A multimodel linear feedback analysis. *Journal of Climate*, 24:2300–2318, 2011. doi: 10.1175/2010JCLI3787.1.

P. Friedlingstein, P. Cox, R. Betts, L. Bopp, W. von Bloh, V. Brovkin, P. Cadule, S. Doney, M. Eby, I. Fung, G. Bala, J. John, C. Jones, F. Joos, T. Kato, M. Kawamiya, W. Knorr, K. Lindsay, H. D. Matthews, T. Raddatz, P. Rayner, C. Reick, E. Roeckner, K.-G. Schnitzler, R. Schnur, K. Strassmann, A. J. Weaver, C. Yoshikawa, and N. Zeng. Climate–Carbon Cycle Feedback Analysis: Results from the C4MIP Model Intercomparison. *Journal of Climate*, 19(14):3337–3353, July 2006. ISSN 0894-8755, 1520-0442. doi: 10.1175/JCLI3800.1.

Veronika Eyring, Sandrine Bony, Gerald A. Meehl, Catherine A. Senior, Bjorn Stevens, Ronald J. Stouffer, and Karl E. Taylor. Overview of the Coupled Model Intercomparison Project Phase 6 (CMIP6) experimental design and organization. *Geoscientific Model Development*, 9(5):1937–1958, May 2016. ISSN 1991-9603. doi: 10.5194/gmd-9-1937-2016.

Peter R. Gent and James C McWilliams. Isopycnal mixing in ocean circulation models. *Journal of Physical Oceanography*, 20:150–160, 1990. doi: 10.1175/1520-0485(1990)020<0150:IMIOCM>2.0.CO;2.

Judith Hauck, Moritz Zeising, Corinne Le Quéré, Nicolas Gruber, Dorothee C. E. Bakker, Laurent Bopp, Thi Tuyet Trang Chau, Özgür Gürses, Tatiana Ilyina, Peter Landschützer, Andrew Lenton, Laure Resplandy, Christian Rödenbeck, Jörg Schwinger, and Roland Séférian. Consistency and Challenges in the Ocean Carbon Sink Estimate for the Global Carbon Budget. *Frontiers in Marine Science*, 7, 2020. ISSN 2296-7745.

Roland Séférian, Sarah Berthet, Andrew Yool, Julien Palmiéri, Laurent Bopp, Alessandro Tagliabue, Lester Kwiatkowski, Olivier Aumont, James Christian, John Dunne, Marion Gehlen, Tatiana Ilyina, Jasmin G. John, Hongmei Li, Matthew C. Long, Jessica Y. Luo, Hideyuki Nakano, Anastasia Romanou, Jörg Schwinger, Charles Stock, Yeray Santana-Falcón, Yohei Takano, Jerry Tjiputra, Hiroyuki Tsujino, Michio Watanabe, Tongwen Wu, Fanghua Wu, and Akitomo Yamamoto. Tracking improvement in simulated marine biogeochemistry between CMIP5 and CMIP6. *Current Climate Change Reports*, 6(3):95–119, August 2020. ISSN 2198-6061. doi: 10.1007/s40641-020-00160-0.

Benjamin Bronselaer, Michael Winton, Joellen Russell, Christopher L Sabine, and Samar Khatiwala. Agreement of CMIP5 simulated and observed ocean anthropogenic CO2 uptake. *Geophysical Research Letters*, 44 (24):12,212–298,305, 2017. doi: 10.1002/2017GL074435.

Weiwei Fu, J. Keith Moore, Francois Primeau, Nathan Collier, Oluwaseun O. Ogunro, Forrest M. Hoffman, and James T. Randerson. Evaluation of Ocean Biogeochemistry and Carbon Cycling in CMIP Earth System Models With the International Ocean Model Benchmarking (IOMB) Software System. *Journal of Geophysical Research: Oceans*, 127(10):e2022JC018965, 2022. ISSN 2169-9291. doi: 10.1029/2022JC018965.

Roland Séférian, Pierre Nabat, Martine Michou, David Saint-Martin, Aurore Voldoire, Jeanne Colin, Bertrand Decharme, Christine Delire, Sarah Berthet, Matthieu Chevallier, Stephane Sénési, Laurent Franchisteguy, Jessica Vial, Marc Mallet, Emilie Joetzjer, Olivier Geoffroy, Jean-François Guérémy, Marie-Pierre Moine, Rym Msadek, Aurélien Ribes, Matthias Rocher, Romain Roehrig, David Salas-y-Mélia, Emilia Sanchez, Laurent Terray, Sophie Valcke, Robin Waldman, Olivier Aumont, Laurent Bopp, Julie Deshayes, Christian Éthé, and Gurvan Madec. Evaluation of CNRM Earth System Model, CNRM-ESM2-1: Role of Earth System Processes in Present-Day and Future Climate. *Journal of Advances in Modeling Earth Systems*, 11(12):4182–4227, 2019. ISSN 1942-2466. doi: 10.1029/2019MS001791.

Xabier Davila, Geoffrey Gebbie, Ailin Brakstad, Siv K. Lauvset, Elaine L. McDonagh, Jörg Schwinger, and Are Olsen. How Is the Ocean Anthropogenic Carbon Reservoir Filled? *Global Biogeochemical Cycles*, 36 (5):e2021GB007055, 2022. ISSN 1944-9224. doi: 10.1029/2021GB007055.

Marina Lévy, Laurent Bopp, P Karleskind, Laure Resplandy, C Ethé, and F Pinsard. Physical pathways for carbon transfers between the surface mixed layer and the ocean interior. *Global Biogeochemical Cycles*, 27 (4):1001–1012, 2013. doi: 10.1002/gbc.20092.

Jean-Baptiste Sallée, Richard J Matear, Stephen R Rintoul, and Andrew Lenton. Localized subduction of anthropogenic carbon dioxide in the Southern Hemisphere oceans. *Nature Geoscience*, 5(8):579–584, 2012. doi: 10.1038/ngeo1523.

Genevieve Jay Brett, Daniel B Whitt, Matthew C Long, Frank O. Bryan, Kate Feloy, and Kelvin J. Richards. Submesoscale Effects on Changes to Export Production Under Global Warming. *Global Biogeochemical Cycles*, 37(3):e2022GB007619, 2023. ISSN 1944-9224. doi: 10.1029/2022GB007619.

Damien Couespel, Marina Lévy, and Laurent Bopp. Oceanic primary production decline halved in eddy-resolving simulations of global warming. *Biogeosciences*, 18(14):4321–4349, July 2021. ISSN 1726-4170. doi: 10.5194/bg-18-4321-2021.

Alexis Bahl, Anand Gnanadesikan, and Marie-aude S Pradal. Scaling global warming impacts on ocean ecosystems: Lessons from a suite of earth system models. *Frontiers in Marine Science*, 7(September), September 2020. ISSN 2296-7745. doi: 10.3389/fmars.2020.00698.

Laure Resplandy, Marina Lévy, and Dennis J McGillicuddy Jr. Effects of Eddy-Driven subduction on ocean biological carbon pump. *Global Biogeochemical Cycles*, 33(8):1071–1084, August 2019. ISSN 0886-6236. doi: 10.1029/2018GB006125.

Cheryl S. Harrison, Matthew C. Long, Nicole S. Lovenduski, and Jefferson K. Moore. Mesoscale Effects on Carbon Export: A Global Perspective. *Global Biogeochemical Cycles*, 32(4):680–703, 2018. ISSN 1944-9224. doi: 10.1002/2017GB005751.

Dhruv Balwada, K. Shafer Smith, and Ryan Abernathey. Submesoscale Vertical Velocities Enhance Tracer Subduction in an Idealized Antarctic Circumpolar Current. *Geophysical Research Letters*, 45(18):9790–9802, 2018. ISSN 1944-8007. doi: 10.1029/2018GL079244.

Amala Mahadevan, A Tagliabue, Laurent Bopp, A Lenton, Laurent Mémery, and Marina Lévy. Impact of episodic vertical fluxes on sea surface pCO2. *Philosophical Transactions of the Royal Society A: Mathematical, Physical and Engineering Sciences*, 369(1943):2009–2025, 2011. doi: 10.1098/rsta.2010.0340.

Eric P Chassignet and Xiaobiao Xu. Impact of horizontal resolution (1/12{\textdegree} to 1/50{\textdegree}) on gulf stream separation, penetration, and variability. *Journal of Physical Oceanography*, 47(8):1999–2021, 2017. doi: 10.1175/JPO-D-17-0031.1.

M. Lévy, P. Klein, A. M. Tréguier, D. Iovino, G. Madec, S. Masson, and K. Takahashi. Modifications of gyre circulation by sub-mesoscale physics. *Ocean Modelling*, 34(1):1–15, January 2010. ISSN 1463-5003. doi: 10.1016/j.ocemod.2010.04.001.

Eric P Chassignet and David P Marshall. Gulf Stream separation in numerical ocean models. *Ocean Modeling in an Eddying Regime. (2008)*, 177:39–61, 2008. doi: 10.1029/177GM05.

Joël J.-M. Hirschi, Bernard Barnier, Claus Böning, Arne Biastoch, Adam T. Blaker, Andrew Coward, Sergey Danilov, Sybren Drijfhout, Klaus Getzlaff, Stephen M. Griffies, Hiroyasu Hasumi, Helene Hewitt, Doroteaciro Iovino, Takao Kawasaki, Andrew E. Kiss, Nikolay Koldunov, Alice Marzocchi, Jennifer V. Mecking, Ben Moat, Jean-Marc Molines, Paul G. Myers, Thierry Penduff, Malcolm Roberts, Anne-Marie Treguier, Dmitry V. Sein, Dmitry Sidorenko, Justin Small, Paul Spence, LuAnne Thompson, Wilbert Weijer, and Xiaobiao Xu. The Atlantic meridional overturning circulation in high resolution models. *Journal of Geophysical Research: Oceans*, January 2020. ISSN 2169-9275. doi: 10.1029/2019JC015522.

Malcolm J. Roberts, Laura C. Jackson, Christopher D. Roberts, Virna Meccia, David Docquier, Torben Koenigk, Pablo Ortega, Eduardo Moreno-Chamarro, Alessio Bellucci, Andrew Coward, Sybren Drijfhout, Eleftheria Exarchou, Oliver Gutjahr, Helene Hewitt, Doroteaciro Iovino, Katja Lohmann, Dian Putrasahan, Reinhard Schiemann, Jon Seddon, Laurent Terray, Xiaobiao Xu, Qiuying Zhang, Ping Chang, Stephen G. Yeager, Frederic S. Castruccio, Shaoqing Zhang, and Lixin Wu. Sensitivity of the Atlantic Meridional Overturning Circulation to Model Resolution in CMIP6 HighResMIP Simulations and Implications for Future Changes. *Journal of Advances in Modeling Earth Systems*, 12(8):e2019MS002014, 2020. ISSN 1942-2466. doi: 10.1029/2019MS002014.

M du Plessis, S Swart, I J Ansorge, and Amala Mahadevan. Submesoscale processes promote seasonal restratification in the Subantarctic Ocean. *Journal of Geophysical Research: Oceans*, 122(4):2960–2975, 2017. doi: 10.1002/2016JC012494.

P Karleskind, Marina Lévy, and Laurent Mémery. Modifications of mode water properties by submesoscales in a bio-physical model of the Northeast Atlantic. *Ocean Modelling*, 39(1):47–60, 2011. doi: 10.1016/j.ocemod.2010.12.003.

Jérôme Chanut, Bernard Barńier, William Large, Laurent Debreu, Thierry Penduff, Jean Marc Molines, and Pierre Mathiot. Mesoscale eddies in the Labrador Sea and their contribution to convection and restratification. *Journal of Physical Oceanography*, 38(8):1617–1643, August 2008. ISSN 00223670. doi: 10.1175/2008JPO3485.1.

Stan Swierczek, Matthew R. Mazloff, Matthias Morzfeld, and Joellen L. Russell. The Effect of Resolution on Vertical Heat and Carbon Transports in a Regional Ocean Circulation Model of the Argentine Basin. *Journal of Geophysical Research: Oceans*, 126(7):e2021JC017235, 2021. ISSN 2169-9291. doi: 10.1029/2021JC017235.

Takaya Uchida, Dhruv Balwada, Ryan P. Abernathey, Galen A. McKinley, Shafer K. Smith, and Marina Lévy. Vertical eddy iron fluxes support primary production in the open Southern Ocean. *Nature Communications*, 11(1):1–8, December 2020. ISSN 20411723. doi: 10.1038/s41467-020-14955-0.

Haidi Chen, Adele K. Morrison, Carolina O. Dufour, and Jorge L. Sarmiento. Deciphering patterns and drivers of heat and carbon storage in the southern ocean. *Geophysical Research Letters*, 46(6):3359–3367, March 2019. ISSN 0094-8276. doi: 10.1029/2018GL080961.

Yusuke Uchiyama, Yota Suzue, and Hidekatsu Yamazaki. Eddy-driven nutrient transport and associated upper-ocean primary production along the Kuroshio. *Journal of Geophysical Research: Oceans*, 122(6):5046–5062, 2017. doi: 10.1002/2017JC012847.

Marina Lévy, D Iovino, Laure Resplandy, Patrice Klein, Gurvan Madec, Anne-Marie Treguier, Sebastien Masson, and Taro Takahashi. Large-scale impacts of submesoscale dynamics on phytoplankton: Local and remote effects. *Ocean Modelling*, 43–44:77–93, 2012. doi: 10.1016/j.ocemod.2011.12.003.

Nathan Beech, Thomas Rackow, Tido Semmler, Sergey Danilov, Qiang Wang, and Thomas Jung. Long-term evolution of ocean eddy activity in a warming world. *Nature Climate Change*, 12(10):910–917, October 2022. ISSN 1758-6798. doi: 10.1038/s41558-022-01478-3.

Josué Martínez-Moreno, Andrew McC. Hogg, Matthew H. England, Navid C. Constantinou, Andrew E. Kiss, and Adele K. Morrison. Global changes in oceanic mesoscale currents over the satellite altimetry record. *Nature Climate Change*, pages 1–7, April 2021. ISSN 1758-678X. doi: 10.1038/s41558-021-01006-9.

Eric C. J. Oliver, Terence J. O'Kane, and Neil J. Holbrook. Projected changes to Tasman Sea eddies in a future climate. *Journal of Geophysical Research: Oceans*, 120(11):7150–7165, November 2015. ISSN 2169-9275. doi: 10.1002/2015JC010993.

Helene Hewitt, Baylor Fox-Kemper, Brodie Pearson, Malcolm Roberts, and Daniel Klocke. The small scales of the ocean may hold the key to surprises. *Nature Climate Change*, 12(6):496–499, June 2022. ISSN 1758-6798. doi: 10.1038/s41558-022-01386-6.

Thomas Rackow, Sergey Danilov, Helge F. Goessling, Hartmut H. Hellmer, Dmitry V. Sein, Tido Semmler, Dmitry Sidorenko, and Thomas Jung. Delayed Antarctic sea-ice decline in high-resolution climate change simulations. *Nature Communications*, 13(1):637, February 2022. ISSN 2041-1723. doi: 10.1038/s41467-022-28259-y.

René M. van Westen and Henk A. Dijkstra. Ocean eddies strongly affect global mean sea-level projections. *Science Advances*, 7(15):eabf1674, April 2021. ISSN 2375-2548. doi: 10.1126/sciadv.abf1674.

Ping Chang, Shaoqing Zhang, Gokhan Danabasoglu, Stephen G. Yeager, Haohuan Fu, Hong Wang, Frederic S. Castruccio, Yuhu Chen, James Edwards, Dan Fu, Yinglai Jia, Lucas C. Laurindo, Xue Liu, Nan Rosenbloom, R. Justin Small, Gaopeng Xu, Yunhui Zeng, Qiuying Zhang, Julio Bacmeister, David A. Bailey, Xiaohui Duan, Alice K. DuVivier, Dapeng Li, Yuxuan Li, Richard Neale, Achim Stössel, Li Wang, Yuan Zhuang, Allison Baker, Susan Bates, John Dennis, Xiliang Diao, Bolan Gan, Abishek Gopal, Dongning Jia, Zhao Jing, Xiaohui Ma, R. Saravanan, Warren G. Strand, Jian Tao, Haiyuan Yang, Xiaoqi Wang, Zhiqiang Wei, and Lixin Wu. An Unprecedented Set of High-Resolution Earth System Simulations for Understanding Multiscale Interactions in Climate Variability and Change. *Journal of Advances in Modeling Earth Systems*, 12(12):e2020MS002298, 2020. ISSN 1942-2466. doi: 10.1029/2020MS002298.

Gurvan Madec, Romain Bourdallé-Badie, Pierre-Antoine Bouttier, Clément Bricaud, Diego Bruciaferri, Daley Calvert, Jérôme Chanut, Emanuela Clementi, Andrew Coward, Damiano Delrosso, Christian Ethé, Simona Flavoni, Tim Graham, James Harle, Doroteaciro Iovino, Dan Lea, Claire Lévy, Tomas Lovato, Nicolas Martin, Sébastien Masson, Silvia Mocavero, Julien Paul, Clément Rousset, Dave Storkey, Andrea Storto, and Martin Vancoppenolle. NEMO ocean engine. *Notes du Pôle de modélisation de l'Institut Pierre-Simon Laplace (IPSL)*, 2017. doi: 10.5281/ZENODO.1472492.

Marina Lévy, A S Krémeur, and Laurent Mémery. Description of the LOBSTER biogeochemical model implemented in the OPA system. Technical report, Laboratoire d'Océanographie Dynamique et de Climatologie - IPSL, 2005.

Rik Wanninkhof. Relationship between wind speed and gas exchange over the ocean. *Journal of Geophysical Research: Oceans*, 97(C5):7373–7382, 1992. doi: 10.1029/92JC00188.

A S Krémeur, Marina Lévy, Olivier Aumont, and G Reverdin. Impact of the subtropical mode water biogeochemical properties on primary production in the North Atlantic: New insights from an idealized model study. *Journal of Geophysical Research: Oceans*, 114(C):C07019, 2009. doi: 10.1029/2008JC005161.

Peter J. Brown, Elaine L. McDonagh, Richard Sanders, Andrew J. Watson, Rik Wanninkhof, Brian A. King, David A. Smeed, Molly O. Baringer, Christopher S. Meinen, Ute Schuster, Andrew Yool, and Marie-José Messias. Circulation-driven variability of Atlantic anthropogenic carbon transports and uptake. *Nature Geoscience*, 14(8):571–577, August 2021. ISSN 1752-0908. doi: 10.1038/s41561-021-00774-5.

S. M. Ridge and G. A. McKinley. Advective controls on the north atlantic anthropogenic carbon sink. *Global Biogeochemical Cycles*, 34(7):1–17, July 2020. ISSN 0886-6236. doi: 10.1029/2019GB006457.

Daniele Iudicone, Keith B. Rodgers, Yves Plancherel, Olivier Aumont, Takamitsu Ito, Robert M. Key, Gurvan Madec, and Masao Ishii. The formation of the ocean's anthropogenic carbon reservoir. *Scientific Reports*, 6 (1):35473, November 2016. ISSN 2045-2322. doi: 10.1038/srep35473.

H. Nakano, M. Ishii, K. B. Rodgers, H. Tsujino, and G. Yamanaka. Anthropogenic CO2 uptake, transport, storage, and dynamical controls in the ocean imposed by the meridional overturning circulation: A modeling study. *Global Biogeochemical Cycles*, 29(10):1706–1724, 2015. ISSN 1944-9224. doi: 10.1002/2015GB005128.

L. C. Jackson, M. J. Roberts, H. T. Hewitt, D. Iovino, T. Koenigk, V. L. Meccia, C. D. Roberts, Y. Ruprich-Robert, and R. A. Wood. Impact of ocean resolution and mean state on the rate of AMOC weakening. *Climate Dynamics*, 55(7):1711–1732, October 2020. ISSN 1432-0894. doi: 10.1007/s00382-020-05345-9.

Michael Winton, Whit G. Anderson, Thomas L. Delworth, Stephen M. Griffies, William J. Hurlin, and Anthony Rosati. Has coarse ocean resolution biased simulations of transient climate sensitivity? *Geophysical Research Letters*, 41(23):8522–8529, December 2014. ISSN 0094-8276. doi: 10.1002/2014GL061523.

J M Gregory, K W Dixon, R J Stouffer, A J Weaver, E Driesschaert, M Eby, Thierry Fichefet, H Hasumi, A Hu, J H Jungclaus, I V Kamenkovich, A Levermann, M Montoya, S Murakami, S Nawrath, A Oka, A P Sokolov, and R B Thorpe. A model intercomparison of changes in the Atlantic thermohaline circulation in response to increasing atmospheric CO 2concentration. *Geophysical Research Letters*, 32(12):n/a—-n/a, 2005. doi: 10.1029/2005GL023209.

Stephen Yeager, Fred Castruccio, Ping Chang, Gokhan Danabasoglu, Elizabeth Maroon, Justin Small, Hong Wang, Lixin Wu, and Shaoqing Zhang. An outsized role for the Labrador Sea in the multidecadal variability of the Atlantic overturning circulation. *Science Advances*, 7(41):eabh3592, October 2021. doi: 10.1126/sciadv.abh3592.

Oliver Gutjahr, Dian Putrasahan, Katja Lohmann, Johann H. Jungclaus, Jin Song Von Storch, Nils Brüggemann, Helmuth Haak, and Achim Stössel. Max planck institute earth system model (MPI-ESM1.2) for the high-resolution model intercomparison project (HighResMIP). *Geoscientific Model Development*, 12(7):3241–3281, July 2019. ISSN 19919603. doi: 10.5194/gmd-12-3241-2019.

Reindert J. Haarsma, Malcolm J. Roberts, Pier Luigi Vidale, Catherine A. Senior, Alessio Bellucci, Qing Bao, Ping Chang, Susanna Corti, Neven S. Fučkar, Virginie Guemas, Jost von Hardenberg, Wilco Hazeleger, Chihiro Kodama, Torben Koenigk, L. Ruby Leung, Jian Lu, Jing-Jia Luo, Jiafu Mao, Matthew S. Mizielinski, Ryo Mizuta, Paulo Nobre, Masaki Satoh, Enrico Scoccimarro, Tido Semmler, Justin Small, and Jin-Song von Storch. High Resolution Model Intercomparison Project (HighResMIP v1.0) for CMIP6. *Geoscientific Model Development*, 9(11):4185–4208, November 2016. ISSN 1991-959X. doi: 10.5194/gmd-9-4185-2016.

Scott D. Bachman. The GM+E closure: A framework for coupling backscatter with the Gent and McWilliams parameterization. *Ocean Modelling*, 136:85–106, April 2019. ISSN 1463-5003. doi: 10.1016/j.ocemod.2019.02.006.

Malte F. Jansen, Alistair Adcroft, Sina Khani, and Hailu Kong. Toward an Energetically Consistent, Resolution Aware Parameterization of Ocean Mesoscale Eddies. *Journal of Advances in Modeling Earth Systems*, 11(8): 2844–2860, 2019. ISSN 1942-2466. doi: 10.1029/2019MS001750.

J. Mak, J. R. Maddison, D. P. Marshall, and D. R. Munday. Implementation of a geometrically informed and energetically constrained mesoscale eddy parameterization in an ocean circulation model. *Journal of Physical Oceanography*, 48(10):2363–2382, 2018. ISSN 15200485. doi: 10.1175/JPO-D-18-0017.1.

Sébastien Barthélémy, Julien Brajard, Laurent Bertino, and François Counillon. Super-resolution data assimilation. *Ocean Dynamics*, 72(8):661–678, August 2022. ISSN 1616-7228. doi: 10.1007/s10236-022-01523-x.

Maike Sonnewald, Redouane Lguensat, Daniel C. Jones, Peter D. Dueben, Julien Brajard, and V. Balaji. Bridging observations, theory and numerical simulation of the ocean using machine learning. *Environmental Research Letters*, 16(7):073008, July 2021. ISSN 1748-9326. doi: 10.1088/1748-9326/ac0eb0.

Laure Zanna and Thomas Bolton. Data-Driven Equation Discovery of Ocean Mesoscale Closures. *Geophysical Research Letters*, 47(17):e2020GL088376, 2020. ISSN 1944-8007. doi: 10.1029/2020GL088376.

Thomas Bolton and Laure Zanna. Applications of Deep Learning to Ocean Data Inference and Subgrid Parameterization. *Journal of Advances in Modeling Earth Systems*, 11(1):376–399, 2019. ISSN 1942-2466. doi: 10.1029/2018MS001472.

Isabela Le Bras, Fiamma Straneo, Morven Muilwijk, Lars H. Smedsrud, Feili Li, M. Susan Lozier, and N. Penny Holliday. How Much Arctic Fresh Water Participates in the Subpolar Overturning Circulation? *Journal of Physical Oceanography*, 51(3):955–973, March 2021. ISSN 0022-3670, 1520-0485. doi: 10.1175/JPO-D-20-0240.1.

Hu Yang, Gerrit Lohmann, Uta Krebs-Kanzow, Monica Ionita, Xiaoxu Shi, Dimitry Sidorenko, Xun Gong, Xueen Chen, and Evan J. Gowan. Poleward shift of the major ocean gyres detected in a warming climate. *Geophysical Research Letters*, 47(5), March 2020. ISSN 0094-8276. doi: 10.1029/2019GL085868.

Camille Lique and Matthew D. Thomas. Latitudinal shift of the Atlantic Meridional Overturning Circulation source regions under a warming climate. *Nature Climate Change*, 8(11):1013–1020, November 2018. ISSN 1758-6798. doi: 10.1038/s41558-018-0316-5.

Ben Bronselaer, Laure Zanna, David R. Munday, and Jason Lowe. The influence of Southern Ocean winds on the North Atlantic carbon sink. *Global Biogeochemical Cycles*, 30(6):844–858, 2016. ISSN 1944-9224. doi: 10.1002/2015GB005364.

Thomas L. Delworth and Fanrong Zeng. Simulated impact of altered southern hemisphere winds on the atlantic meridional overturning circulation. *Geophysical Research Letters*, 35(20):L20708, October 2008. ISSN 0094-8276. doi: 10.1029/2008GL035166.

Stephanie A. Henson, Charlotte Laufkötter, Shirley Leung, Sarah L. C. Giering, Hilary I. Palevsky, and Emma L. Cavan. Uncertain response of ocean biological carbon export in a changing world. *Nature Geoscience*, 15 (4):248–254, April 2022. ISSN 1752-0908. doi: 10.1038/s41561-022-00927-0.

C. Laufkötter, M. Vogt, N. Gruber, M. Aita-Noguchi, O. Aumont, L. Bopp, E. Buitenhuis, S. C. Doney, J. Dunne, T. Hashioka, J. Hauck, T. Hirata, J. John, C. Le Quéré, I. D. Lima, H. Nakano, R. Seferian, I. Totterdell, M. Vichi, and C. Völker. Drivers and uncertainties of future global marine primary production in marine ecosystem models. *Biogeosciences*, 12(23):6955–6984, December 2015. ISSN 1726-4170. doi: 10.5194/bg-12-6955-2015.

Tim DeVries. The oceanic anthropogenic CO2 sink: Storage, air-sea fluxes, and transports over the industrial era. *Global Biogeochemical Cycles*, 28(7):631–647, 2014. ISSN 1944-9224. doi: 10.1002/2013GB004739.

Ben Bronselaer and Laure Zanna. Heat and carbon coupling reveals ocean warming due to circulation changes. *Nature*, 584(7820):227–233, August 2020. ISSN 14764687. doi: 10.1038/s41586-020-2573-5.

Lester Kwiatkowski, Olivier Torres, Laurent Bopp, Olivier Aumont, Matthew Chamberlain, James R. Christian, John P. Dunne, Marion Gehlen, Tatiana Ilyina, Jasmin G. John, Andrew Lenton, Hongmei Li, Nicole S. Lovenduski, James C. Orr, Julien Palmieri, Yeray Santana-Falcón, Jörg Schwinger, Roland Séférian, Charles A. Stock, Alessandro Tagliabue, Yohei Takano, Jerry Tjiputra, Katsuya Toyama, Hiroyuki Tsujino, Michio Watanabe, Akitomo Yamamoto, Andrew Yool, and Tilo Ziehn. Twenty-first century ocean warming, acidification, deoxygenation, and upper-ocean nutrient and primary production decline from CMIP6 model projections. *Biogeosciences*, 17(13):3439–3470, July 2020. ISSN 1726-4189. doi: 10.5194/bg-17-3439-2020.